

Photon-counting statistics of the degenerate optical parametric oscillator

Reeta Vyas and Surendra Singh

Department of Physics, University of Arkansas, Fayetteville, Arkansas 72701

(Received 22 May 1989)

Nonclassical light beams generated by the degenerate optical parametric oscillator operating below threshold are analyzed in terms of photoelectron-counting sequences. The positive- P representation is used to calculate the generating function for photoelectron statistics in a closed form. This generating function is used to derive expressions for the photoelectron-counting and waiting-time distributions. The dependence of these distributions on mean photon number inside the cavity and efficiency of detection is studied. The relationship between photoelectron-counting sequence and the photon emission sequence is used to present a simple physical picture of light beams produced by the degenerate parametric oscillator.

I. INTRODUCTION

Squeezed states of light have been observed in a variety of physical systems.¹⁻³ These states do not admit a positive nonsingular diagonal representation in terms of coherent states and are, therefore, an example of nonclassical states of the electromagnetic field. Since squeezing only refers to the variance of the two quadrature components of the electric field, it does not fully characterize these states. With experimental realization of these states, increasing attention is being paid to their quantum-statistical properties.^{4,5} These properties for idealized squeezed states are well known.⁶⁻⁹ The systems in which squeezed states have been observed experimentally are dissipative nonlinear systems, and photon statistical properties of squeezed states produced by these systems have received much less attention.

The largest amount of squeezing has been observed in an optical parametric oscillator (OPO) operating below threshold.^{2,3} This simple dissipative quantum system has played an important role in recent studies of squeezing. In an OPO (Ref. 10) a strong pump beam interacts with a nonlinear crystal and is frequency down-converted into two beams of smaller frequencies inside an optical cavity. If the two beams produced in down conversion have the same frequency, then the oscillator is termed a degenerate parametric oscillator (DPO); otherwise it is termed a nondegenerate parametric oscillator (NDPO). A quantum-mechanical treatment of the OPO is of course essential since it generates light with nonclassical properties.

For an oscillator a distinction must be made between intracavity photon statistics and the statistics of photons emitted by the cavity. Intracavity statistics are not directly observable. The statistics of photons emitted by the cavity can be measured in photon-counting experiments. The statistics of the field inside and outside the cavity are, of course, related. Many recent studies of the quantum-statistical properties of the DPO have centered around the calculation of the spectrum of squeezing^{11,12} inside and outside the cavity because of the subtleties involved in the detection of squeezed light. Intracavity

field statistics were discussed by Drummond, McNeil, and Walls¹³ by using the complex- P representation and by Graham by using the Wigner function¹³. More recently, Wolinsky and Carmichael^{4,14} have provided a complete description of the quantum-statistical properties of the intracavity field by using the positive- P representation. For the photons escaping the cavity, the mean and variance of photon counts have also been calculated by Collett and Loudon.¹⁵

In this paper we discuss the quantum-statistical properties of photon beams generated by an OPO as measured by a detector placed outside the cavity. These properties can be studied in photoelectric-counting and correlation experiments with low-intensity light beams appropriate for an OPO below threshold. From the measured photoelectron statistics, photon statistics of the incident light beam can be derived. For a detector of unit efficiency each photodetection corresponds to an emission of a photon by the cavity. In this case, the photoelectric-counting sequence and the photon emission sequence are equivalent. We begin by expressing the photoelectron-counting statistics in terms of a generating function in Sec. II. The statistics of the waiting time between successive photoelectric counts can also be derived from the same generating function. In Sec. III the c number equations of motion for the DPO operating below threshold are presented. This is done by using the positive- P representation. The solutions to these c -number equations are used to obtain a closed form expression for the generating function. From this generating function exact expressions for the photoelectron-counting distribution and the waiting-time distribution are derived in Sec. IV. Intracavity photon statistics are discussed in Sec. V. We conclude by summarizing the principal results of the paper in Sec. VI.

II. THE GENERATING FUNCTION

Consider a photoelectric detector illuminated by a stationary weak beam of light. The probability $p(m, T)$ of detecting m photoelectric counts at the output of the detector in a time interval T is given by¹⁶

$$p(m, T) = \left\langle \mathcal{T} : \frac{1}{m!} \left[\eta \int_0^T \hat{I}(t) dt \right]^m \exp \left[-\eta \int_0^T \hat{I}(t) dt \right] : \right\rangle, \quad (1)$$

where $0 \leq \eta \leq 1$ is the efficiency of detection and $\hat{I}(t)$ is the photon-flux operator expressed in units of photons per second. The colons denote normal ordering of the enclosed operator product and \mathcal{T} stands for time ordering of the operators to the right. The angular brackets in Eq. (1) denote the expectation value with respect to the state of the incident light beam. The photoelectric-counting distribution $p(m, T)$ can be derived from the generating function

$$G(s, T) = \left\langle \mathcal{T} : \exp \left[-s \eta \int_0^T \hat{I}(t) dt \right] : \right\rangle. \quad (2)$$

Note that $G(1, T) = p(0, T)$ so that $G(1, T)$ is the probability that no photoelectric counts are registered in time T . In terms of $G(s, T)$, we can write

$$p(m, T) = \frac{(-1)^m}{m!} \left[\frac{d^m}{ds^m} G(s, T) \right]_{s=1} \quad (3)$$

and the factorial moments

$$\langle m^{(r)} \rangle = \langle m(m-1) \cdots (m-r+1) \rangle$$

of m can be derived from

$$\langle m^{(r)} \rangle = (-1)^r \left[\frac{d^r}{ds^r} G(s, T) \right]_{s=0}. \quad (4)$$

Another quantity of interest in describing the photoelectron-counting sequence is the waiting-time distribution $w(T)$ such that $w(T)dT$ is the probability that the waiting time between successive photoelectron counts lies between T and $T+dT$. This distribution is given by^{8,17}

$$w(T) = \eta \left\langle \mathcal{T} : \hat{I}(T) \exp \left[-s \eta \int_0^T \hat{I}(t) dt \right] \hat{I}(0) : \right\rangle / \langle \hat{I} \rangle \quad (5)$$

and is related to $G(s, T)$ by

$$w(T) = \frac{1}{\eta \langle \hat{I} \rangle} \frac{d^2}{dT^2} G(1, T) \quad (6)$$

for a stationary beam of light. In general, higher-order waiting-time distribution functions are needed to describe photoelectron-counting sequences. Here we will concentrate only on $w(T)$. Once the generating function $G(s, T)$ is known, the photoelectron statistics and photoelectron waiting-time distributions can be calculated from Eqs. (3), (4), and (6).

III. EQUATIONS OF MOTION

Consider two quantized modes of a cavity having frequencies 2ω and ω and interacting with each other via an intracavity nonlinear crystal. The high-frequency mode, termed the pump mode, is excited by an injected classical signal. In the interaction picture the Hamiltonian for

this system with perfect phase matching is given by¹³

$$\hat{H} = \frac{1}{2} i \hbar (\kappa \hat{a}^{\dagger 2} \hat{b} - \kappa^* \hat{a}^2 \hat{b}^{\dagger}) + i \hbar \Gamma (\epsilon \hat{b}^{\dagger} - \epsilon^* \hat{b}) + \hat{H}_{\text{loss}}, \quad (7)$$

where κ is the mode-coupling constant which can be expressed in terms of the third-order nonlinear susceptibility of the crystal and certain integrals over mode functions, \hat{b} and \hat{b}^{\dagger} are the creation and annihilation operators for the pump mode, and \hat{a} and \hat{a}^{\dagger} are the creation and annihilation operators for the subharmonic mode. The dimensionless classical-field amplitude ϵ is defined in such a way that $|\epsilon|^2$ gives the number of photons incident on the cavity in one lifetime of the cavity $(2\Gamma)^{-1}$ at the pump frequency. Decays of cavity modes are introduced in the usual way by coupling cavity modes to zero-temperature reservoirs and a Markov master equation for the density matrix describing the coupled cavity modes is derived. This equation is converted into an equivalent set of classical Langevin equations by introducing an appropriate phase-space representation of the density matrix. The familiar coherent-state diagonal representation is not useful in this case because it does not lead to a Fokker-Planck equation with positive-definite diffusion. This difficulty is removed by the use of the positive- P representation¹⁸ which leads to a Fokker-Planck equation. The corresponding Langevin equations for the subharmonic mode, below threshold, where pump depletion is negligible, are^{13,14}

$$\dot{\alpha} = -\gamma \alpha + \kappa \epsilon \alpha_* + \sqrt{\kappa \epsilon} \xi_1(t), \quad (8)$$

$$\dot{\alpha}_* = -\gamma \alpha_* + \kappa \epsilon \alpha + \sqrt{\kappa \epsilon} \xi_2(t), \quad (9)$$

where $(2\gamma)^{-1}$ is the cavity lifetime at the subharmonic frequency. The Langevin noise terms $\xi_1(t)$ and $\xi_2(t)$ are two statistically independent real Gaussian white-noise processes with zero mean and unit intensity and α and α_* are two complex variables associated with the operators \hat{a} and \hat{a}^{\dagger} , respectively, in the positive- P representation. If $\hat{\rho}$ represents the density matrix for the subharmonic field, then the phase-space density \mathcal{P} in the positive- P representation is introduced by¹⁸

$$\hat{\rho} = \int \int_{\mathcal{D}} d^2\alpha d^2\alpha_* \frac{|\alpha\rangle\langle\alpha_*|}{\langle\alpha_*|\alpha\rangle} \mathcal{P}(\alpha, \alpha_*), \quad (10)$$

where \mathcal{D} is some suitably chosen domain in the four-dimensional phase space spanned by the complex variables α and α_* , so that $\mathcal{P}(\alpha, \alpha_*)$ is real, positive, and normalized to unity. The complex variables α and α_* are associated with the operators \hat{a} and \hat{a}^{\dagger} by $\hat{a}|\alpha\rangle = \alpha|\alpha\rangle$ and $\langle\alpha_*|\hat{a}^{\dagger} = \alpha_*\langle\alpha_*|$. Unlike the diagonal representation α and α_* are not complex conjugates of each other. This means that Eqs. (8) and (9) describe trajectories in a four-dimensional phase space. By means of the positive- P function the normally ordered operator averages can be calculated as c -number averages according to the correspondence

$$\langle \hat{a}^{\dagger m} \hat{a}^n \rangle = \int \int_{\mathcal{D}} d^2\alpha d^2\alpha_* \alpha_*^m \alpha^n \mathcal{P}(\alpha, \alpha_*). \quad (11)$$

Since Eqs. (8) and (9) are equivalent to the Fokker-Planck

equation for $\mathcal{P}(\alpha, \alpha_*)$, the averages such as those in Eq. (11) may be carried out with respect to the trajectories of Eqs. (8) and (9). By writing $\kappa\varepsilon = |\kappa\varepsilon|e^{-i\phi}$ and introducing new variables x and y by

$$\begin{aligned}\alpha &= xe^{-i\phi/2}, \\ \alpha_* &= ye^{-i\phi/2},\end{aligned}\quad (12)$$

we find that Eqs. (8) and (9) can be rewritten as

$$\dot{x} = -\gamma x + \kappa\varepsilon y + \sqrt{|\kappa\varepsilon|}\xi_1(t), \quad (13)$$

$$\dot{y} = -\gamma y + \kappa\varepsilon x + \sqrt{|\kappa\varepsilon|}\xi_2(t). \quad (14)$$

These equations ensure that in the steady state the variables x and y are real because any imaginary parts to them decay away. These equations also preserve x and y as real quantities if they are real initially. The initial state of the oscillator, when it is turned on, is the vacuum state with $x=0=y$ and this is sufficient to guarantee that x and y will stay real for all times. If we introduce new real variables by

$$\begin{aligned}u_1 &= \frac{x+y}{2}, \quad u_2 = \frac{x-y}{2}, \\ \lambda_1 &= (\gamma - |\kappa\varepsilon|), \quad \lambda_2 = (\gamma + |\kappa\varepsilon|), \\ q_1(t) &= \frac{\xi_2 + \xi_1}{\sqrt{2}}, \quad q_2(t) = \frac{\xi_1 - \xi_2}{\sqrt{2}},\end{aligned}\quad (15)$$

the coupled set of equations [(6) and (7)] leads to the following uncoupled equations for the random variables u_1 and u_2 :

$$\dot{u}_1 = -\lambda_1 u_1 + \sqrt{|\kappa\varepsilon|/2} q_1(t), \quad (16)$$

$$\dot{u}_2 = -\lambda_2 u_2 + \sqrt{|\kappa\varepsilon|/2} q_2(t). \quad (17)$$

The threshold of oscillation is at $|\kappa\varepsilon| = \gamma$ so that below threshold $|\kappa\varepsilon| < \gamma$ and both decay constants λ_1 and λ_2 are positive. The noise processes $q_1(t)$ and $q_2(t)$ are real Gaussian white-noise processes with

$$\langle q_i(t) \rangle = 0, \quad \langle q_i(t) q_j(t') \rangle = \delta_{ij} \delta(t-t'). \quad (18)$$

The steady-state solutions to Eqs. (16) and (17) are

$$u_1(t) = \left[\frac{|\kappa\varepsilon|}{2} \right]^{1/2} \int_{-\infty}^t dt' e^{-\lambda_1(t-t')} q_1(t'), \quad (19)$$

$$u_2(t) = \left[\frac{|\kappa\varepsilon|}{2} \right]^{1/2} \int_{-\infty}^t dt' e^{-\lambda_2(t-t')} q_2(t'). \quad (20)$$

It follows from Eqs. (17)–(20) that the variables $u_1(t)$ and $u_2(t)$ are statistically independent real Gaussian random variables with mean and variance given by

$$\begin{aligned}\langle u_i(t) \rangle &= 0, \\ \langle u_i(t) u_j(t') \rangle &= \frac{1}{4} \frac{|\kappa\varepsilon|}{\lambda_i} \delta_{ij} e^{-\lambda_i |t-t'|}.\end{aligned}\quad (21)$$

The variables u_1 and u_2 have a simple interpretation in terms of the unsqueezed and squeezed quadrature components of the subharmonic fields produced by the DPO.

Let us introduce Hermitian operators

$$\begin{aligned}\hat{X}_{1\phi} &= \frac{\hat{a}e^{-i\phi/2} + \hat{a}^\dagger e^{i\phi/2}}{2}, \\ \hat{X}_{2\phi} &= \frac{\hat{a}e^{-i\phi/2} - \hat{a}^\dagger e^{i\phi/2}}{2i},\end{aligned}\quad (22)$$

where the phase angle ϕ is defined in Eq. (12). Normally ordered moments of $\hat{X}_{j\phi}$ can be evaluated by using Eqs. (11), (12), (15), and (19)–(21). We find for the mean,

$$\begin{aligned}\langle \hat{X}_{1\phi} \rangle &= \langle u_1 \rangle = 0, \\ \langle \hat{X}_{2\phi} \rangle &= -i \langle u_2 \rangle = 0,\end{aligned}\quad (23)$$

and for the normally ordered variance, with $\Delta\hat{X}_{j\phi} = \hat{X}_{j\phi} - \langle \hat{X}_{j\phi} \rangle$,

$$\begin{aligned}\langle :(\Delta\hat{X}_{1\phi})^2: \rangle &= \langle (\Delta u_1)^2 \rangle = \frac{1}{4} \frac{|\kappa\varepsilon|}{\lambda_1}, \\ \langle :(\Delta\hat{X}_{2\phi})^2: \rangle &= -\langle (\Delta u_2)^2 \rangle = -\frac{1}{4} \frac{|\kappa\varepsilon|}{\lambda_2}.\end{aligned}\quad (24)$$

Thus the variables u_1 and $-iu_2$ correspond, respectively, to the unsqueezed and squeezed quadrature components $\hat{X}_{1\phi}$ and $\hat{X}_{2\phi}$ in the positive- P representations. With solutions (19) and (20) we can now evaluate the generating function $G(s, T)$. First we note that positive- P allows us to evaluate normally ordered averages as c -number averages so that

$$G(s, T) = \left\langle \exp \left[-s\eta \int_0^T I(t) dt \right] \right\rangle, \quad (25)$$

where $I(t) = 2\gamma\alpha\alpha_*$ is the photon-number flux variable for the photons emitted by the cavity. The average in Eq. (25) is to be evaluated with respect to the trajectories of the variables α and α_* . Using Eqs. (12), (15), and (19)–(21) in Eqs. (25) we find that the generating function can be written as the product

$$G(s, T) = Q_1(s, T) Q_2(s, T), \quad (26)$$

where

$$Q_1(s, T) = \left\langle \exp \left[-2s\eta\gamma \int_0^T u_1^2(t) dt \right] \right\rangle, \quad (27)$$

$$Q_2(s, T) = \left\langle \exp \left[2s\eta\gamma \int_0^T u_2^2(t) dt \right] \right\rangle. \quad (28)$$

The factorization in Eq. (26) occurs because $u_1(t)$ and $u_2(t)$ are statistically independent random processes. The problem of the evaluation of the generating function now reduces to the evaluation of $Q_1(s, T)$ and $Q_2(s, T)$. Since $u_1(t)$ and $u_2(t)$ are Gaussian processes with exponential correlation functions, both $Q_1(s, T)$ and $Q_2(s, T)$ can be evaluated in closed form following the method of Slepian.¹⁹ Principal steps in this derivation are outlined in the Appendix. The results for $Q_1(s, T)$ and $Q_2(s, T)$ are

$$Q_1(s, T) = \frac{e^{\lambda_1 T/2}}{\left[\cosh(z_1 T) + \frac{1}{2} \left[\frac{\lambda_1 + z_1}{z_1 + \lambda_1} \right] \sinh(z_1 T) \right]^{1/2}}, \quad (29)$$

$$Q_2(s, T) = \frac{e^{\lambda_2 T/2}}{\left[\cosh(z_2 T) + \frac{1}{2} \left(\frac{\lambda_2}{z_2} + \frac{z_2}{\lambda_2} \right) \sinh(z_2 T) \right]^{1/2}}, \quad (30)$$

where

$$\begin{aligned} z_1^2 &= \lambda_1^2 + 2s\eta\gamma\kappa\varepsilon, \\ z_2^2 &= \lambda_2^2 - 2s\eta\gamma\kappa\varepsilon. \end{aligned} \quad (31)$$

Note that the variable z_1 is always real. For physical parameters the variable z_2 is also real. This ensures that $Q_2(s, T)$ is well defined for all values of T . Equations (26) and (29)–(31) determine the generating function for the DPO below threshold. We now proceed to discuss photon-counting statistics.

IV. PHOTOELECTRON-COUNTING STATISTICS

Substituting Eq. (26) into Eq. (1) and using the Leibnitz rule to carry out the differentiation, we find that the probability $p(m, T)$ of counting m photons in time T can be written as

$$\begin{aligned} p(m, T) &= \frac{(-1)^m}{m!} \sum_{r=0}^m \binom{m}{r} \left[\left[\frac{d^{m-r}}{ds^{m-r}} Q_1(s, T) \right] \right. \\ &\quad \left. \times \left[\frac{d^r}{ds^r} Q_2(s, T) \right] \right]_{s=1} \\ &= \sum_{r=0}^m p_1(m-r, T) p_2(r, T), \end{aligned} \quad (32)$$

where $p_j(r, T)$ for $j=1, 2$ are given by

$$\begin{aligned} p_j(r, T) &= \frac{(-1)^r}{r!} \left[\frac{d^r}{ds^r} Q_j(s, T) \right]_{s=1} \\ &= \sum_{k=1}^r \left[\frac{2r-k}{r} \right] D_j^{(k)}(1) p_j(r-k, T). \end{aligned} \quad (33)$$

The last relation allows us to evaluate $p_j(r, T)$ recursively. The coefficients $D_j^{(k)}(s)$ are given by

$$\begin{aligned} D_j^{(k)}(s) &= \frac{1}{2} Q_j^2(s, T) e^{-\lambda_j T} \left[T \frac{dz_j}{ds} \right]^k \frac{(-1)^{k+1}}{k!} \\ &\quad \times \left[\frac{z_j T}{2} \left[\frac{\lambda_j}{z_j} + \frac{z_j}{\lambda_j} \right] i_k(z_j T) \right. \\ &\quad \left. + z_j T \left[1 + \frac{k}{\lambda_j T} \right] i_{k-1}(z_j T) \right], \end{aligned} \quad (34)$$

where $i_k(x)$ are modified spherical Bessel functions.²⁰ A similar procedure using Eq. (4) yields factorial moments of the photon-counting distribution in the form

$$\begin{aligned} \langle m^{(r)} \rangle &= (-1)^r \left[\frac{d^r}{ds^r} Q_1(s, T) Q_2(s, T) \right]_{s=0} \\ &= \sum_{k=0}^r \binom{r}{k} \langle m_1^{(k)} \rangle \langle m_2^{(r-k)} \rangle, \end{aligned} \quad (35)$$

where

$$\begin{aligned} \langle m_j^{(r)} \rangle &= (-1)^r \left[\frac{d^r}{ds^r} Q_j(s, T) \right]_{s=0} \\ &= \sum_{k=0}^{r-1} \frac{r!}{k!} \left[\frac{r+k}{r} \right] D_j^{(r-k)}(0) \langle m_j^{(k)} \rangle. \end{aligned} \quad (36)$$

Once again the last relation allows us to evaluate $\langle m_j^{(r)} \rangle$ recursively. The factorization that occurs in Eqs. (32) and (36) once again reflects the statistical independence of the variables u_1 and u_2 . Equations (32) and (36) have a formal similarity to the corresponding expressions for a partially polarized thermal light beam^{21,22} and it is tempting to interpret Eq. (32) to mean that the cavity emits two types of photons. The total number of photons m recorded in the time interval T may then be interpreted as coming from various combinations of these two types of photons. This interpretation, however, is incorrect because both $p_1(m, T)$ and $p_2(m, T)$ in Eq. (32) cannot be interpreted as probabilities; the function $p_1(m, T)$ is a true probability, but the function $p_2(m, T)$ becomes negative for odd values of its argument m . This has interesting consequences for the forms of $p(m, T)$ as will be seen shortly. Thus, although the expressions in Eq. (32) and (35) are formally similar to those for a thermal light beam, their physical content is quite different.

The waiting-time distribution $w(T)$ is obtained by using Eqs. (26), (29), and (30) in Eq. (6). We find it convenient to rewrite the generating function $G(s, T)$ in the form

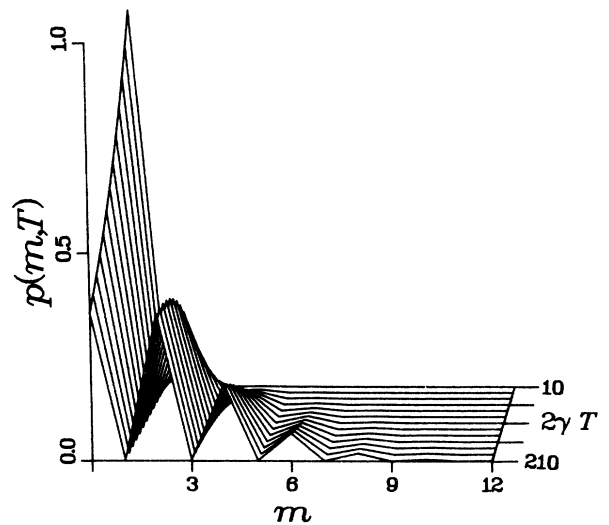


FIG. 1. Photoelectron-counting probability $p(m, T)$ as a function of m and the counting interval T for small-mean-photon-number $\bar{n}=0.01$. The curves are meaningful only for integer values of m .

$$G(s, T) = [(1 - A_1)(1 - A_2)]^{1/2} \frac{e^{(2\gamma - z_1 - z_2)T/2}}{[(1 - A_1 e^{-2z_1 T})(1 - A_2 e^{-2z_2 T})]^{1/2}}, \quad (37)$$

where

$$A_1 = \left[\frac{z_1 - \lambda_1}{z_1 + \lambda_1} \right]^2, \quad (38)$$

$$A_2 = \left[\frac{z_2 - \lambda_2}{z_2 + \lambda_2} \right]^2.$$

We then obtain

$$\begin{aligned} w(T) &= (2\gamma\eta\bar{n})^{-1} G(1, T) \\ &\times \left[\left[\frac{1}{2}(z_1 + z_2 - 2\gamma) + \frac{z_1 A_1}{e^{2z_1 T} - A_1} + \frac{z_2 A_2}{e^{2z_2 T} - A_2} \right]^2 \right. \\ &\quad \left. + 2 \frac{z_1^2 A_1 e^{2z_1 T}}{(e^{2z_1 T} - A_1)^2} + 2 \frac{z_2^2 A_2 e^{2z_2 T}}{(e^{2z_2 T} - A_2)^2} \right] \quad (39) \end{aligned}$$

for the waiting-time distribution, where z_1 and z_2 are given by Eqs. (31) with $s=1$. We can also obtain the probability $P_1(T)$ that the first photodetection occurs at a time T after counting is started arbitrarily at time $t=0$. This probability is given by⁸

$$\begin{aligned} P_1(T) &= -\frac{d}{dt} G(1, T) \\ &= G(1, T) \left[\frac{1}{2}(z_1 + z_2 - 2\gamma) \right. \\ &\quad \left. + \frac{z_1 A_1}{e^{2z_1 T} - A_1} + \frac{z_2 A_2}{e^{2z_2 T} - A_2} \right]. \quad (40) \end{aligned}$$

The counting distribution, together with waiting-time distribution, provides a clear picture of photoelectric-counting sequence. When the detector has unit detection efficiency $\eta=1$ each photoelectric count corresponds to an emitted photon. In this case the photoelectric pulse sequence is a true representative of the photon sequence emitted by the cavity. If the efficiency of detection is less than unity $\eta < 1$, the photoelectric pulse sequence is related to the photon emission sequence only indirectly. We consider the $\eta=1$ and < 1 cases separately.

A. Unit detection efficiency $\eta=1$

In this case we can speak of photoelectric counts registered by the detector and photons emitted by the cavity interchangeably because each photon emitted by the cavity is registered by the detector as a photoelectric count. The counting distribution $p(m, T)$ exhibits a variety of shapes depending on the value of the parameter $|\kappa\epsilon|/\gamma$ and the counting interval T . The parameter $0 \leq |\kappa\epsilon|/\gamma \leq 1$ is related to the mean photon number \bar{n} inside the cavity by

$$\bar{n} = \langle \alpha_* \alpha \rangle = \frac{1}{2} \left[\frac{|\kappa\epsilon|^2}{\gamma^2 - |\kappa\epsilon|^2} \right]. \quad (41)$$

The counting distribution $p(m, T)$ for low-mean-photon-number \bar{n} is shown in Fig. 1 as a function of m for several different values of the counting interval T . It will be seen that for short counting times T such that $2\gamma T < 1$ [counting time T less than $T_c = (2\gamma)^{-1}$, the cavity lifetime] $p(m, T)$ monotonically decreases as m increases. For longer counting intervals $2\gamma T > 1$ the counting distribution shows even-odd oscillations. The probability of counting an odd number of photons is small compared to the probability of counting an even number of photons. The depth of these modulations increases with increasing counting interval and in the limit $2\gamma T \gg 1$ the odd counting probabilities become negligible compared to the even counting probabilities. These oscillations in $p(m, T)$ can be understood in terms of the fundamental process of generation of photons inside the cavity. Photons are produced simultaneously in pairs^{23,24} inside the cavity in the process of frequency down conversion. These photons escape the cavity independently with a lifetime of the order of the cavity lifetime $T_c = (2\gamma)^{-1}$. For long counting times $2\gamma T > 1$, there is a preponderance of even photon counts because both photons from each pair eventually escape the cavity. In the steady state the mean rate of production of photons inside the cavity equals the mean rate $2\gamma\bar{n}$ of photons escaping the cavity. At low-mean-photon-number $\bar{n} \ll 1$, photon pairs are created inside the cavity at an average rate $\gamma\bar{n}$ corresponding to an average pair separation $T_p = (\gamma\bar{n})^{-1}$. Once a pair is created inside, both photons escape the cavity within a time of the order T_c , long before another pair is produced. The cavity is quiescent for long periods of the order of T_p and emits only for short durations of the order of T_c whenever a pair of photons is created. Outside the cavity, therefore, photons appear to be coming out in pairs with photons in a pair separated from each other, on the average, by a time of the order of T_c and each such photon pair separated from the next one by an average time T_p . The qualitative picture presented here is the one that naturally emerges from Eqs. (32) and (39) in this regime of low-mean-photon-number \bar{n} . For $\bar{n} \ll 1$ and $2\gamma T \gg 1$, the generating function $G(s, T)$ has the form

$$G(s, T) \approx \left[1 - \frac{\bar{n}}{2} s^2 \right] \exp[-\langle m \rangle / 2 + \langle m \rangle (s-1)^2 / 2]. \quad (42)$$

This equation leads to the following expressions for the counting probabilities:

$$p(2m, T) \approx \left[1 - \frac{\bar{n}}{2} \left[1 + \frac{2m}{\langle m \rangle} \right] \right] \frac{1}{m!} \left[\frac{\langle m \rangle}{2} \right]^m e^{-\langle m \rangle / 2}, \quad (43)$$

$$p(2m+1, T) \approx \bar{n} \frac{1}{m!} \left[\frac{\langle m \rangle}{2} \right]^m e^{-\langle m \rangle/2}, \quad (44)$$

where

$$\langle m \rangle = \eta 2\gamma \bar{n} T \quad (45)$$

is the mean number of photons detected in the interval T . Note that since $\bar{n} \ll 1$, odd counting probabilities are negligible. The even counting probabilities [Eq. (43)] then define a Poisson distribution of photon pairs emitted at random by the cavity at an average rate $\gamma \bar{n}$ pairs per second corresponding to the mean number of pairs in T equal to $\gamma \bar{n} T = \langle m \rangle / 2$. We may then introduce the probability $\mathcal{P}(r, T)$ that the cavity emits r photon pairs in the interval T by

$$\mathcal{P}(r, T) = \frac{1}{r!} \left[\frac{\langle m \rangle}{2} \right]^r e^{-\langle m \rangle/2}. \quad (46)$$

The approximate expressions [(43) and (44)] are compared with the exact distribution (32) in Fig. 2. It is found that Eqs. (43) and (44) provide a good approximation to the exact counting probabilities for $\bar{n} \leq 0.02$ ($|\kappa\epsilon|/\gamma < 0.1$) and $2\gamma T \gg 1$.

The interpretation of photons emitted by the cavity in terms of photon pairs also emerges from the waiting-time distribution $w(T)$ which describes the time interval T between a photon detected at time t and the next detected at time $t+T$. This distribution derived from Eq. (39) is shown in Fig. 3. There are two distinct time scales visible in $w(T)$. This can be seen more quantitatively with the help of the following approximate expression for $w(T)$ which can be derived from Eq. (39) when \bar{n} is small. This expression is

$$w(T) \approx 2\gamma \bar{n} e^{-\gamma \bar{n} T} \left[\frac{1}{4}(1 + e^{-4\gamma T}) + \frac{1}{2} \left[3 + \frac{1}{\bar{n}} \right] e^{-2\gamma T} \right], \quad (47)$$

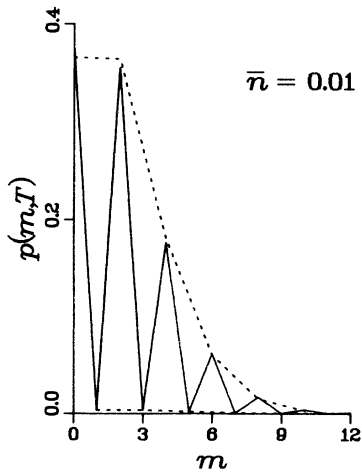


FIG. 2. Comparison of the exact counting probability (full curve) with the approximation (dotted curve) given by Eqs. (43) and (44) for $\bar{n} = 0.01$ and $2\gamma T = 200$. The curves are meaningful only for integer values of m .

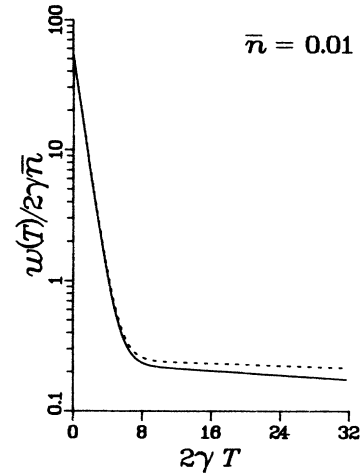


FIG. 3. Photoelectron waiting-time distribution $w(T)$ as a function of the waiting-time T . The full curve is Eq. (39) and the dotted curve is Eq. (47).

where we have kept enough terms in \bar{n} so that $\int_0^\infty w(T) dT = 1 + O(\bar{n})$ and $w(0)/2\gamma\bar{n}$ gives the correct value for the normalized normally ordered second moment of the light intensity. Equation (47) is shown by the dotted curve in Fig. 3 and is found to be a good approximation to the exact result. The short time scale $T_c = (2\gamma)^{-1}$ corresponds to the mean separation of photons in a pair and the long time constant $T_p = (\gamma\bar{n})^{-1}$ corresponds to the average separation of successive photon pairs emitted by the cavity. The value of $w(T)$ for $2\gamma T \ll 1$ is related to the normalized second moment of the light intensity by

$$w(T) = 2\gamma \bar{n} \langle \alpha_*(T) \alpha(T) \alpha_*(0) \alpha(0) \rangle / \langle \alpha_* \alpha \rangle^2 \equiv 2\gamma \bar{n} g^{(2)}(T), \quad (48)$$

so that $w(0)/2\gamma\bar{n}$ is a direct measure of the bunching effect exhibited by photons emitted by the DPO. For thermal light fields $w(0)/2\gamma\bar{n} = 2$, but for the DPO the emitted photons exhibit much greater bunching.

As the pump amplitude increases, \bar{n} grows and the above picture changes. With increasing pump strength photon pairs are copiously produced inside the cavity. The mean cavity photon number \bar{n} grows and during any counting interval, photons from many pairs created inside contribute to the photon flux from the cavity and it is no longer possible to speak of photon pairs escaping the cavity. Although the counting distribution $p(m, T)$ still shows even-odd oscillations for large counting times $2\gamma T > 1$, the even-odd modulations are smaller. An example of $p(m, T)$ for a large-cavity photon number \bar{n} is shown in Fig. 4. It is not possible to derive a simple expression for $p(m, T)$ in this regime except in the short-counting-time limit. When $2\gamma T \ll 1$ we obtain the following approximation for the generating function:

$$G(s, T) = [1 + 2\bar{n} - 2\bar{n}(s\gamma\eta T - 1)^2]^{-1/2}. \quad (49)$$

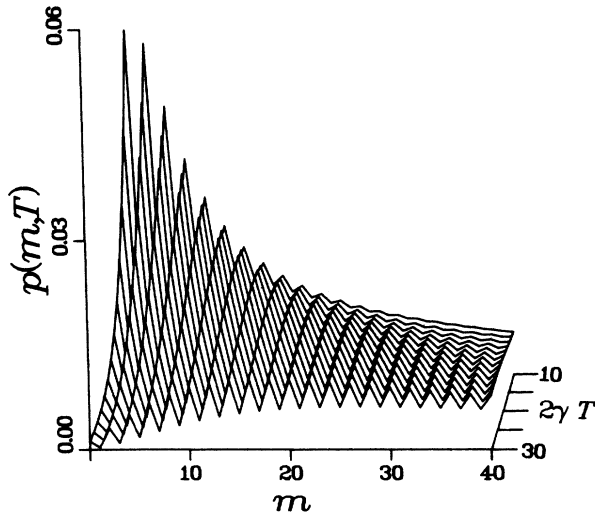


FIG. 4. Photoelectron-counting probability $p(m, T)$ for large-mean-photon-number $\bar{n}=5$. The curves are meaningful only for integer values of m .

For \bar{n} not too small we can derive the following expression for $p(m, T)$:

$$p(m, T) \approx \frac{(2m-1)!!}{m!} \frac{\langle m \rangle^m}{(1+2\langle m \rangle)^{m+1/2}} \quad (50)$$

This expression is compared with the exact counting distribution in Fig. 5 and is found to be a very good approximation.

The waiting-time distribution for the large \bar{n} regime is shown in Fig. 6. The time scale $T_c = (2\gamma)^{-1}$ is suppressed. The dominant time scale in this case is the mean separation time $T_s = (2\gamma\bar{n})^{-1}$ between photons emitted by the cavity. This is the so-called high-degeneracy

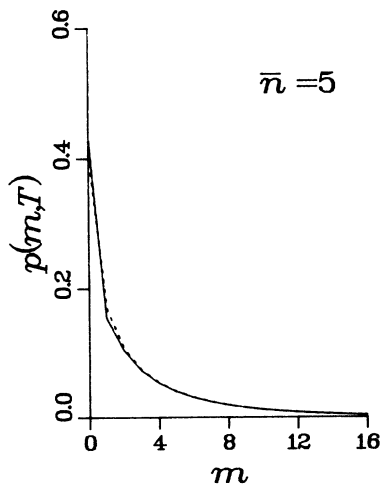


FIG. 5. Comparison of the exact counting probability $p(m, T)$ (full curve) and the approximation (dotted curve) given by Eq. (50) for short counting times in the large-mean-photon-number limit $\bar{n}=5$ and $2\gamma T=0.5$. The curves are meaningful only for integer values of m .

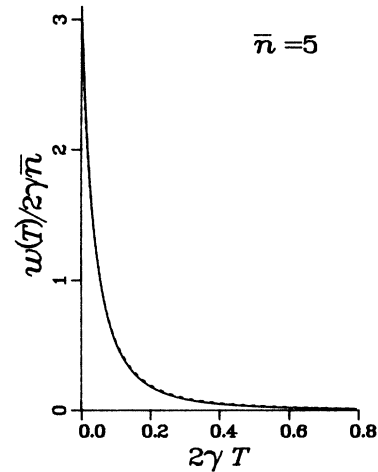


FIG. 6. Comparison of the exact waiting-time distribution $w(T)$ (full curve) with the approximation (dashed curve) given by Eq. (51) in the large-mean-photon-number (high-degeneracy) limit $\bar{n}=5$.

limit that was discussed in Ref. 8. In this limit, $\bar{n} \gg 1$, we arrive at the following expression for $w(T)$:

$$w(T) = 2\gamma\bar{n} \frac{3}{(1+4\gamma\bar{n}T)^{5/2}} \quad (51)$$

which reproduces exact distribution for all values of T for which $w(T)$ is not too small. This distribution agrees with the corresponding distribution for an ideal squeezed state in the high-degeneracy limit.⁸ The dotted curve in Fig. 6 shows Eq. (51).

B. Nonunit detection efficiency $\eta < 1$

When the detection efficiency is less than unity we must distinguish between the photon emission sequence from the cavity and the photoelectric-counting sequence recorded by the detector. This is because not every photon emitted by the cavity is recorded as a photoelectric count. The nonunit detection efficiency is equivalent to converting the photo-emission sequence into a photoelectric pulse sequence by randomly selecting the detected photons.

The effect of nonunit detection efficiency on $p(m, T)$ is shown in Figs. 7(a) and 7(b) for small- and large-mean-photon-number \bar{n} . It will be seen that with decreasing detection efficiency the even-odd oscillations begin to fade and for $\eta \ll 1$, they are completely washed out. This is because at low detection efficiencies both photons from a pair may not be detected. For $\bar{n} \ll 1$ we can arrive at the following expression for $G(s, T)$ when η is small:

$$G(s, T) \approx \exp[-\langle m \rangle / 2 + \langle m \rangle (s\eta - 1)^2 / 2] \quad (52)$$

Using this result in Eq. (3) we find

$$p(m, T) = \sum_{r=[m/2]}^{\infty} \binom{2r}{m} \eta^m (1-\eta)^{2r-m} \rho(r, T) \quad (53)$$

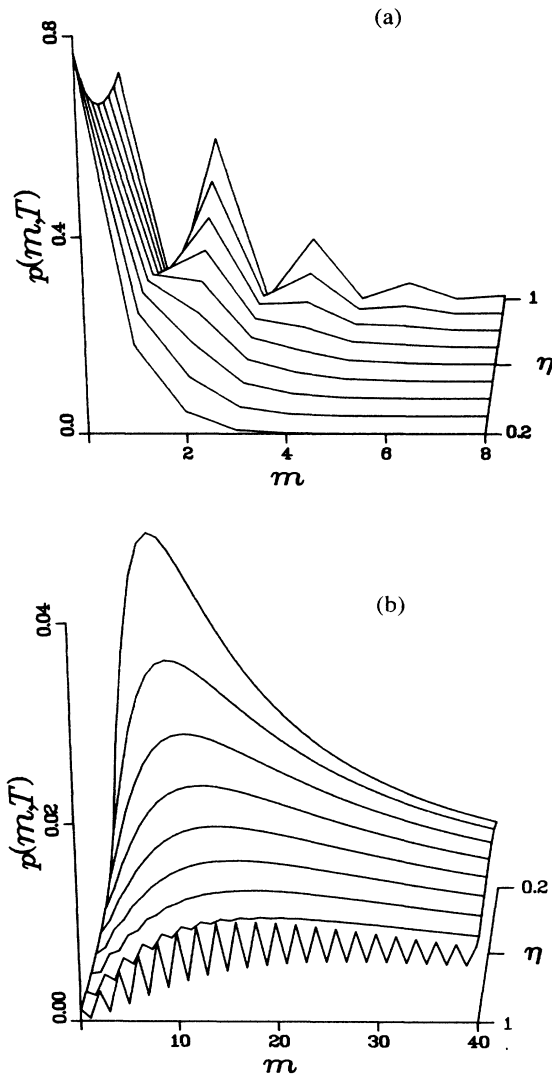


FIG. 7. Effect of nonunit detection efficiency η on the counting probability $p(m, T)$ in the low- and high-mean-photon-number limits: (a) $\bar{n} = 0.01$, $2\gamma T = 150$; (b) $\bar{n} = 5$, $2\gamma T = 30$. The curves are meaningful only for integer values of m .

where $[m/2]$ is equal to $m/2$ for even m and $(m + 1)/2$ for odd m . Here $\mathcal{A}(r, T)$ which is given by Eq. (46) is the probability that r photon pairs are emitted by the cavity in time T . Equation (53) has a natural interpretation in terms of photon pairs emitted by the cavity. Each term in Eq. (53) is proportional to the pair emission probability $\mathcal{A}(r, T)$. These r pairs have $2r$ photons. Out of these $2r$ photons m photons can be selected in $\binom{2r}{m}$ ways and each selection has the probability $\eta^m(1-\eta)^{2r-m}$. Thus, although the even-odd oscillations die out for nonunit detection efficiency, the structure of the photoelectric-counting probability still suggests an interpretation in terms of photon pairs emitted by the cavity. However, the concept of photon pairs cannot be introduced based on the observed counting probabilities. At sufficiently

low detection efficiency photoelectric pulses are recorded essentially randomly from the photon sequence emitted by the cavity at a rate $\eta 2\gamma \bar{n}$, much lower than the rate $2\gamma \bar{n}$ at which photons are emitted by the cavity. For large-mean-photon numbers the counting probability does not have a simple expression.

The effect of nonunit detection efficiency $\eta < 1$ on the photoelectron waiting-time distribution is shown in Fig. 8. The distribution $w(T)$ does not, in general, have a simple form. However, in the limit $\eta \ll 1$ we find that for short waiting times

$$w(T) = \eta 2\gamma \bar{n} \left[1 + \frac{e^{-\lambda_1 T}}{8\lambda_1^2 \bar{n}^2} + \frac{e^{-\lambda_2 T}}{8\lambda_2^2 \bar{n}^2} \right] \equiv \eta 2\gamma \bar{n} g^{(2)}(T), \tag{54}$$

so that $w(T)$ is essentially the second-order normalized intensity correlation function. For long waiting times $w(T)$ decays exponentially as expected for a random sequence of photons. In the low-detection efficiency limit the waiting distribution $w(T)/\eta 2\gamma \bar{n}$ simply becomes the probability of recording one photoelectric count at time t and another count at time $t + T$.

Before leaving this section we comment on the multiplicative factor 2γ that occurs in the definition of photon flux [Eq. (25)]. This factor was introduced in Eqs. (8) and (9) to denote the rate at which the cavity loses photons at the subharmonic frequency to all loss mechanisms, including absorption inside the crystal and the cavity mirrors, scattering, and, of course, the mirror transmission. Only the mirror transmission loss contributes to photon flux from the cavity. The factor 2γ should then be replaced by $2\gamma\eta'$, where η' ($0 \leq \eta' \leq 1$) is the ratio of transmission loss to the total loss. This factor denotes the efficiency with which photons that are lost by the cavity are collected for detection. This factor can be incorporated into the definition of the detection efficiency. For a two-port cavity, the factor η' should be reduced further unless photons escaping from both ends of the cavity are collected for detection.

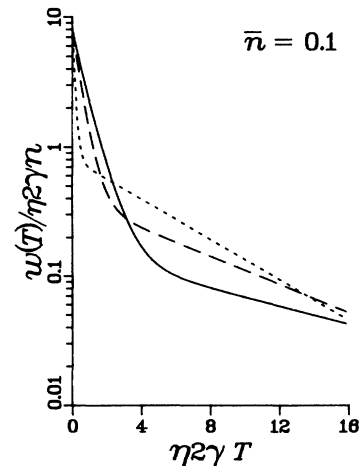


FIG. 8. Effect of nonunit detection efficiency η on the waiting-time distribution function $w(T)$. Full curve, $\eta = 1$; dashed curve, $\eta = 0.5$; dotted curve, $\eta = 0.1$.

V. INTRACAVITY PHOTON STATISTICS

In this section we discuss the cavity photon occupation probability $P(n)$ such that $P(n)$ is the probability that the cavity contains n photons in the steady state. Although $P(n)$ is not directly measurable, it is interesting to compare its form with the photon-counting probability $p(m, T)$ which, of course, is directly measurable in photoelectric-counting experiments. An expression for $P(n)$ can be derived as follows. First we note that $P(n) = \langle n | \hat{\rho} | n \rangle$ so that from Eqs. (10) and (12) we find

$$P(n) = \int_{-\infty}^{\infty} dx \int_{-\infty}^{\infty} dy \frac{(xy)^n}{n!} e^{-xy} \mathcal{P}(x, y), \quad (55)$$

where the positive- P function $\mathcal{P}(x, y)$ is given from Eqs. (12), (15), and (19)–(21) to be⁴

$$\mathcal{P}(x, y) = \frac{1}{2\bar{n}} \exp \left[2xy - \left(\frac{1+2\bar{n}}{2\bar{n}} \right)^{1/2} (x^2 + y^2) \right]. \quad (56)$$

Substituting Eq. (55) into (54) and carrying out the integrals we obtain the following expression for $P(n)$:

$$P(n) = \frac{1}{2^n} \left[\frac{2}{2+3\bar{n}} \right]^{1/2} \left[\frac{\sqrt{2\bar{n}}}{2\sqrt{1+2\bar{n}} - \sqrt{2\bar{n}}} \right]^n \times \sum_{r=0}^n (-1)^r \frac{(2r-1)!!}{r!} \frac{(2n-2r-1)!!}{(n-r)!} \times \left[\frac{2\sqrt{1+2\bar{n}} - \sqrt{2\bar{n}}}{2\sqrt{1+2\bar{n}} + \sqrt{2\bar{n}}} \right]^r, \quad (57)$$

where $n!! = n(n-2)(n-4) \dots$ with $-1!! = 1$. On introducing the generating function $F(s)$ by

$$F(s) = \sum_{n=0}^{\infty} s^n P(n) = \frac{1}{[1+2\bar{n}-2\bar{n}(1-s/2)^2]^{1/2}}, \quad (58)$$

we can write $P(n)$ and its factorial moments in a more compact form,

$$P(n) = \frac{(-1)^n}{n!} \left[\frac{d^n}{ds^n} F(s) \right]_{s=1}, \quad (59)$$

$$\langle n^{(r)} \rangle = \frac{(-1)^r}{n!} \left[\frac{d^r}{ds^r} F(s) \right]_{s=0}. \quad (60)$$

Here \bar{n} is the mean photon number inside the cavity. The intracavity photon-number distribution $P(n)$ depends only on the mean photon number inside the cavity. The distribution $P(n)$ is shown in Fig. 9 for several different values of \bar{n} . It will be seen that unlike the photoelectric-counting distribution, $P(n)$ does not show even-odd oscillations. This, however, is not surprising since $P(n)$ refers to the probability that the cavity contains n photons at any given time in the steady state.⁵ The cavity is losing photons continuously even as they are being created in pairs. Therefore, at any instant it may contain any number, even or odd, of photons. The situation is different in the transient regime where $P(n)$, which now depends on time t that has elapsed since the oscillator was turned on, may show even-odd oscillation in its passage towards the

steady state.⁵

An interesting feature of $P(n)$ in the steady state is that for large values of \bar{n} it exhibits long tails indicating large intensity fluctuations. Relative intensity fluctua-

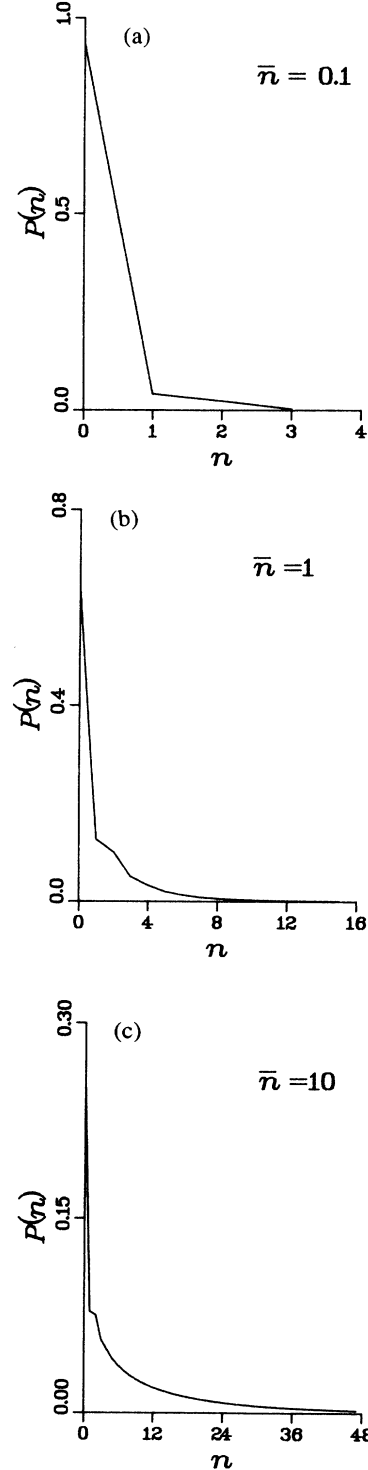


FIG. 9. Intracavity photon-number distribution $P(n)$ as a function of n for several different values of \bar{n} . The curves are meaningful only for integer values of n .

tions as measured by $g^{(2)}(0)$, however, decrease and approach a value of 3 as the oscillator threshold is approached. In terms of bunching of photons the photon beams produced by the DPO are always more bunched than the photon beams from a thermal source. Another interesting feature is that the ratios $P(1)/P(0)$ and $P(2)/P(1)$ approach values $\frac{1}{3}$ and 1, respectively. This steplike behavior is clearly seen in Fig. 9. This behavior continues for larger values of n , but the step size becomes progressively smaller. For large values of n the distribution decays slowly to zero.

In terms of intracavity photon-number distribution we can derive another expression for the photoelectric-counting distribution $p(m, T)$. Let β denote the probability of detecting a photon, then $p(m, T)$ is given by

$$p(m, T) = \sum_{n=m}^{\infty} \binom{n}{m} \beta^m (1-\beta)^{n-m} P(n). \quad (61)$$

Using Eqs. (57) and (58) we can write Eq. (61) in the form

$$p(m, T) = \frac{(-1)^m}{m!} \left[\frac{d^m}{ds^m} F(\beta s) \right]_{s=1}, \quad (62)$$

where $F(\beta s)$ is given by Eq. (58) with s replaced by βs . The single-photon detection probability $\beta(T)$ is a complicated function of T . For short times, however, $\beta(T) = 2\gamma \bar{n} T$. Substituting this in Eq. (62) and using Eq. (58) we recover the short-time approximation [Eq. (49)] for the photoelectron-counting statistics.

We close this section by giving the intracavity photon-number distribution when pump depletion is taken into account. The corresponding positive- P distribution, which is valid both below and above threshold, has been derived by Wolinsky and Carmichael.⁴ This distribution is

$$P(x, y) = \text{const} \times [(\sigma - x^2)(\sigma - y^2)]^{n_0 - 1} e^{2xy}, \quad |x|, |y| \leq \sqrt{\sigma}, \quad (63)$$

where $\sigma = 2\Gamma\epsilon/\kappa$ and $n_0 = 2\Gamma\gamma/\kappa^2$. Here $(2\gamma)^{-1}$ and $(2\Gamma)^{-1}$ are the cavity lifetimes at the subharmonic and the pump frequencies. Using this expression in Eq. (55) we obtain

$$P(2r) = \frac{\sigma^{2r}}{(2r)!} \sum_{m=0}^{\infty} \frac{\sigma^{2m}}{(2m)!} \left[\frac{\Gamma(r+m+\frac{1}{2})}{\Gamma(r+m+n_0+\frac{1}{2})} \right]^2 / \sum_{m=0}^{\infty} \frac{\sigma^{2m}}{(2m)!} \left[\frac{\Gamma(m+\frac{1}{2})}{\Gamma(m+n_0+\frac{1}{2})} \right]^2, \quad (64)$$

$$P(2r+1) = \frac{\sigma^{2r+1}}{(2r+1)!} \sum_{m=0}^{\infty} \frac{\sigma^{2m+1}}{(2m+1)!} \left[\frac{\Gamma(r+m+\frac{3}{2})}{\Gamma(r+m+n_0+\frac{3}{2})} \right]^2 / \sum_{m=0}^{\infty} \frac{\sigma^{2m}}{(2m)!} \left[\frac{\Gamma(m+\frac{1}{2})}{\Gamma(m+n_0+\frac{1}{2})} \right]^2, \quad (65)$$

Examples of $P(n)$ derived from Eqs. (64) and (65) are shown in Fig. 10. The exact distribution below and at threshold is shown in Figs. 10(a) and 10(b), and qualitatively reproduces the behavior of Eq. (57). Above threshold, where Eq. (57) is not valid, new features appear. One noteworthy feature is the appearance of two most probable values of n just above threshold in Fig. 10(c). The distribution also exhibits a tendency to oscillate for small values of n . High above threshold the distribution is centered at a nonzero value of n indicating finite amplitude of oscillations

VI. SUMMARY AND CONCLUSIONS

We have studied the photoelectron-counting sequences and photon emission sequences from the degenerate parametric oscillator cavity below threshold. These sequences are described in terms of the counting distribution $p(m, T)$ and the waiting-times distribution $w(T)$ between successive photoemissions or detections. The expressions derived in this paper are valid for arbitrary counting time and detection efficiency.

For low excitation of the cavity ($\bar{n} \ll 1$), the photon emission sequence may be described in terms of pairs of photons emitted by the cavity. The average separation between photons in a pair is of the order of the cavity lifetime $T_c = (2\gamma)^{-1}$. The separation between pairs of

photons is of the order of the inverse of the mean rate of emission of photons by the cavity. These photon pairs outside eventually reflect the pair production of photons inside the cavity. The role of cavity in the low-photon-number regime is to stretch the photon pair correlations to a time of the order of T_c .

It is interesting to compare the field produced by a thermal source with the field produced by the DPO. The field produced by a thermal source can be described as two real independent Gaussian random processes with the same variance and spectral properties. The field produced by the DPO can also be described by two real independent Gaussian processes, u_1 and u_2 . However, these two variables have different variance and spectral properties. It is this difference that is responsible for the very different behavior of photon statistics in the two cases.

The approach presented in this paper provides an example of the power and usefulness of the positive- P representation in describing nonlinear dissipative quantum systems. The techniques presented here are also applicable to many other systems such as the nondegenerate parametric oscillator and four-wave mixers. Since the equations describing intracavity degenerate four-wave mixing, under appropriate conditions, are equivalent to the equations for the DPO, the results of this paper are directly applicable to intracavity degenerate four-wave mixer.¹²

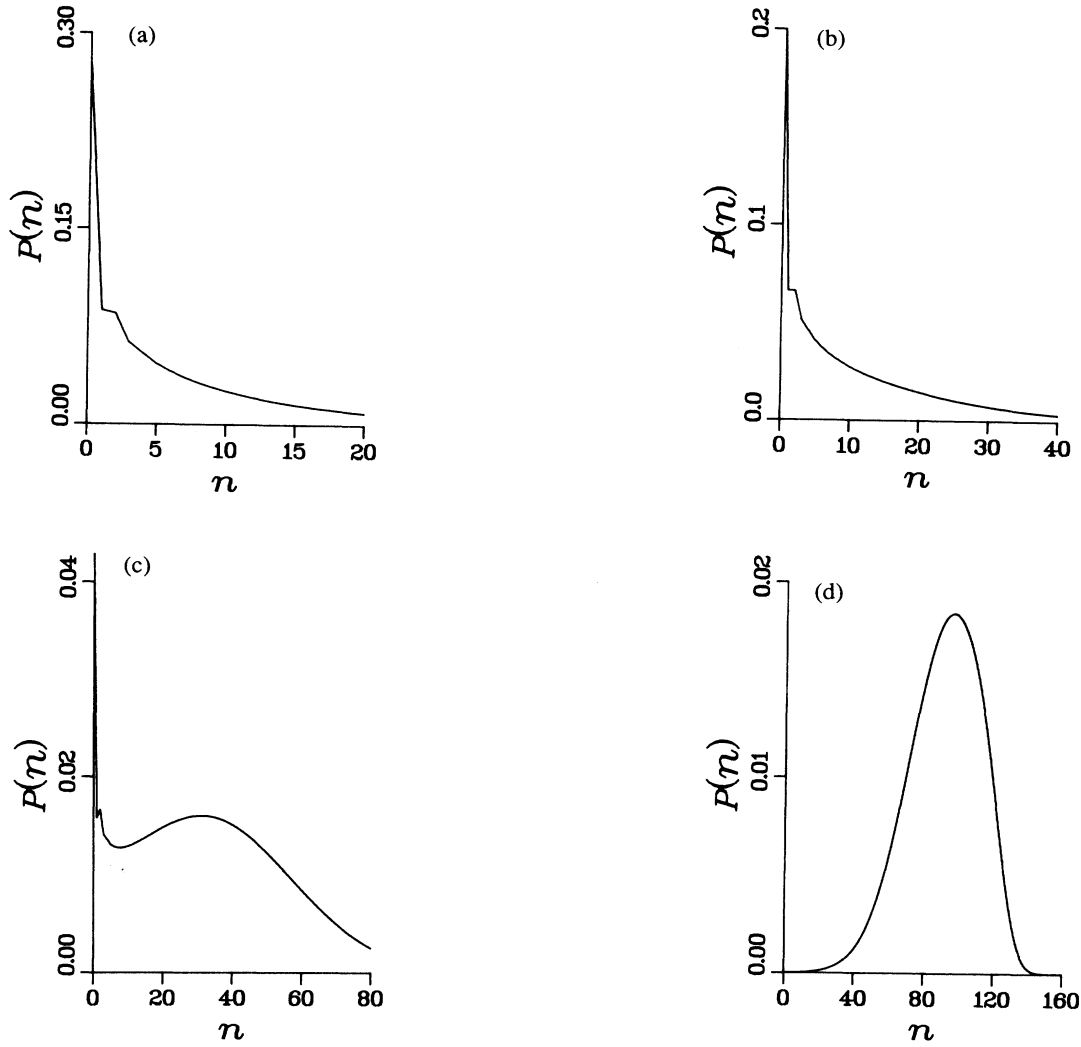


FIG. 10. Exact intracavity photon-number distribution, with pump depletion included, for (a) below threshold $\sigma=980$, (b) at threshold $\sigma=1000$, (c) slightly above threshold $\sigma=1040$, and (d) high above threshold $\sigma=1100$ operation of the oscillator with $n_0=1000$. The curves are meaningful only for integer values of n .

Similarly, the results for the nondegenerate optical parametric oscillator are applicable to intracavity nondegenerate four-wave mixer.

ACKNOWLEDGMENTS

This paper was based upon work supported in part by the National Science Foundation.

APPENDIX

In order to evaluate the generating function, we make a Karhunen-Loève expansion²⁵ of the random variable $u_1(t)$ in the interval $0 \leq t \leq T$ as

$$u_1(t) = \frac{1}{2} \left[\frac{|\kappa \epsilon|}{\lambda_1} \right]^{1/2} \sum_{n=1}^{\infty} \beta_n \phi_n(t), \quad (\text{A1})$$

where the coefficients β_n are random variables and the

functions $\phi_n(t)$ satisfy the integral eigenvalue equation

$$\int_0^T e^{-\lambda_1|t-t'|} \phi_n(t') dt' = \mu_n \phi_n(t). \quad (\text{A2})$$

Since the kernel $e^{-\lambda_1|t-t'|}$ is real symmetric and positive definite the eigenvalues $\mu_1 \geq \mu_2 \geq \dots$ are real and positive and the eigenfunctions $\phi_n(t)$ can be chosen to form an orthonormal set

$$\int_0^T \phi_n(t) \phi_m(t) dt = \delta_{nm}. \quad (\text{A3})$$

Furthermore, since $u_1(t)$ is a real Gaussian process and $\phi_n(t)$ are orthonormal, the coefficients β_n are independent real Gaussian random variables with zero mean and variance μ_n given by

$$\langle \beta_n^2 \rangle = \mu_n. \quad (\text{A4})$$

Using Eqs. (A1), (A3), and (A4) in Eq. (27) we find

$$Q_1(s, T) = \prod_{n=1}^{\infty} \left[\frac{1}{1 + s\eta\gamma|\kappa\epsilon|\mu_n/\lambda_1} \right]^{1/2}. \tag{A5}$$

The integral eigenvalue equation (A2) can be converted into the differential eigenvalue equation

$$\frac{d^2}{dt^2} \phi_n(t) + \omega_n^2 \phi_n(t) = 0, \tag{A6}$$

where

$$\omega_n^2 = \frac{2\lambda_1}{\mu_n} - \lambda_1^2. \tag{A7}$$

The eigenvalues μ_n are now determined in terms of ω_n . Solutions of Eq. (A6) satisfy Eq. (A2) provided ω_n are chosen to be the roots of

$$f(\omega) = \cos\omega T + \frac{1}{2} \left[\frac{\lambda_1}{\omega} - \frac{\omega}{\lambda_1} \right] \sin\omega T = 0. \tag{A8}$$

The roots of this equation are real and occur in pairs $\pm\omega_1, \pm\omega_2, \dots$, with $0 < \omega_1 < \omega_2 < \dots$, and form an unbounded sequence. Expressed in terms of ω_n , Eq. (A5) reads as

$$Q_1(s, T) = \prod_{n=1}^{\infty} \left[\frac{\omega_n^2 + \lambda_1^2}{\omega_n^2 + \lambda_1^2 + 2s\eta|\kappa\epsilon|\gamma} \right]^{1/2}. \tag{A9}$$

Taking the logarithmic derivative of $Q_1(s, T)$ with respect to s we obtain

$$\frac{1}{Q_1(s, T)} \frac{dQ_1(s, T)}{ds} = -\eta|\kappa\epsilon|\gamma \sum_{n=0}^{\infty} \frac{1}{\omega_n^2 + \lambda_1^2 + 2s\eta|\kappa\epsilon|\gamma}. \tag{A10}$$

In order to evaluate this sum we note that the function $f(\omega)$ [Eq. (A8)], considered as a function of a complex variable ω , has simple zeros at $\pm\omega_n$ and $\lim_{n \rightarrow \infty} \omega_n$ is unbounded. Furthermore, $f(\omega)$ is analytic for all values of ω so that it may be written as the infinite product²⁶

$$f(\omega) = \prod_{n=1}^{\infty} (\omega - \omega_n)(\omega + \omega_n). \tag{A11}$$

Its logarithmic derivative with respect to ω ,

$$\frac{d}{d\omega} \ln f(\omega) = \sum_{n=1}^{\infty} \left[\frac{1}{\omega - \omega_n} + \frac{1}{\omega + \omega_n} \right], \tag{A12}$$

has singularities which are simple poles at $\omega = \pm\omega_n$ with residue $+1$. It follows from Eqs. (A8) and (A12) that the singularities of the function

$$F(\omega) = \frac{1}{\omega^2 + \lambda_1^2 + 2s\eta|\kappa\epsilon|\gamma} \frac{d}{d\omega} \times \ln \left[\cos\omega T + \frac{1}{2} \left[\frac{\lambda_1}{\omega} - \frac{\omega}{\lambda_1} \right] \sin\omega T \right], \tag{A13}$$

are simple poles at $\omega = \pm i(\lambda_1^2 + 2s\eta|\kappa\epsilon|\gamma)^{1/2}$ and $\omega = \pm\omega_n$. Now consider the contour integral $\oint_{C_n} F(\omega) d\omega$, where C_n is a circle of radius R_n ($\omega_n < R_n < \omega_{n+1}$) centered at the origin and not passing through any pole. Then $R_n \rightarrow \infty$ as $n \rightarrow \infty$ so that as $R_n \rightarrow \infty$ the contour will enclose all the poles of $F(\omega)$. Now as $n \rightarrow \infty$, the integral $\oint_{C_n} F(\omega) d\omega$ is $O(R_n^{-2})$ and so tends to zero as n tends to infinity. This means that the sum of the residues at the poles of $F(\omega)$ vanishes and we obtain

$$2 \sum_{n=1}^{\infty} \frac{1}{\omega_n^2 + z_1^2} - \frac{1}{z_1} \frac{d}{dz_1} \ln \left[\cosh(z_1 T) + \frac{1}{2} \left[\frac{\lambda_1}{z_1} + \frac{z_1}{\lambda_1} \right] \sinh(z_1 T) \right] = 0. \tag{A14}$$

Using this result in Eq. (A10) and integrating we find¹⁹

$$Q_1(s, T) = \frac{e^{\lambda_1 T/2}}{\left[\cosh(z_1 T) + \frac{1}{2} \left[\frac{\lambda_1}{z_1} + \frac{z_1}{\lambda_1} \right] \sinh(z_1 T) \right]^{1/2}}, \tag{A15}$$

where

$$z_1^2 = \lambda_1^2 + 2s\eta\gamma|\kappa\epsilon|. \tag{A16}$$

Using a similar procedure we find $Q_2(s, T)$ is given by

$$Q_2(s, T) = \frac{e^{\lambda_2 T/2}}{\left[\cosh(z_2 T) + \frac{1}{2} \left[\frac{\lambda_2}{z_2} + \frac{z_2}{\lambda_2} \right] \sinh(z_2 T) \right]^{1/2}}, \tag{A17}$$

where

$$z_2^2 = \lambda_2^2 - 2s\eta\gamma|\kappa\epsilon|. \tag{A18}$$

- ¹Special issue on squeezed states of light, *J. Opt. Soc. Am. B* **4**, 10 (1987).
- ²L. Wu, H. J. Kimble, J. L. Hall, and H. Wu, *Phys. Rev. Lett.* **57**, 2520 (1986).
- ³P. Grangier, R. E. Slusher, B. Yurke, and A. LaPorta, *Phys. Rev. Lett.* **59**, 2153 (1987).
- ⁴M. J. Wolinsky and H. J. Carmichael, *Phys. Rev. Lett.* **60**, 1836 (1988).
- ⁵Reeta Vyas and Surendra Singh, *Opt. Lett.* (to be published); in *Coherence and Quantum Optics VI*, edited by J. H. Eberly, L. Mandel, and E. Wolf (Plenum, New York, 1989).
- ⁶H. P. Yuen, *Phys. Rev. A* **13**, 2226 (1976).
- ⁷W. Schleich and J. A. Wheeler, *J. Opt. Soc. Am. B* **4**, 1715 (1987).
- ⁸Reeta Vyas and Surendra Singh, *Phys. Rev. A* **38**, 2423 (1988).
- ⁹J. Huang and P. Kumar, *Bull. Am. Phys. Soc.* **33**, 1671 (1988); *Phys. Rev. A* **40**, 1760 (1989).
- ¹⁰For a review of optical parametric oscillators and amplifiers, see R. G. Smith, in *Laser Handbook*, edited by F. T. Arecchi and E. O. Schulz-Duboise (North-Holland, Amsterdam, 1972), Vol. I, p. 837.
- ¹¹M. J. Collett and C. W. Gardiner, *Phys. Rev. A* **30**, 1386 (1984); 3761 (1985); C. W. Gardiner and C. M. Savage, *Opt. Commun.* **50**, 173 (1984).
- ¹²M. J. Collett and D. F. Walls, *Phys. Rev. A* **32**, 2887 (1985); C. M. Savage and D. F. Walls, *J. Opt. Soc. Am. B* **4**, 1514 (1987).
- ¹³P. D. Drummond, K. J. McNeil, and D. F. Walls, *Opt. Acta* **28**, 211 (1980); R. Graham, in *Quantum Statistics in Optics and Solid-State Physics*, Vol. 66 of *Springer Tracts in Modern Physics* (Springer-Verlag, Berlin, 1973).
- ¹⁴H. J. Carmichael and M. J. Wolinsky, in *Quantum Optics IV*, edited by J. D. Harvey and D. F. Walls (Springer-Verlag, Berlin, 1986), pp. 208–220.
- ¹⁵M. J. Collett and R. Loudon, *J. Opt. Soc. Am. B* **4**, 1525 (1987).
- ¹⁶P. L. Kelley and W. H. Kleiner, *Phys. Rev.* **136**, A316 (1964).
- ¹⁷H. J. Carmichael, Surendra Singh, Reeta Vyas, and P. R. Rice, *Phys. Rev. A* **39**, 1200 (1989).
- ¹⁸P. D. Drummond and C. W. Gardiner, *J. Phys. A* **13**, 2353 (1980).
- ¹⁹D. Slepian, *Bell System Tech. J.* **37**, 163 (1958).
- ²⁰G. Arfken, *Mathematical Methods for Physicists* (Academic, New York, 1985), Chap. 11.
- ²¹A. K. Jaiswal and C. L. Mehta, *Phys. Rev.* **186**, 1355 (1969).
- ²²G. Bedard, *Phys. Rev.* **151**, 1038 (1966).
- ²³D. C. Burnham and D. L. Weinberg, *Phys. Rev. Lett.* **25**, 84 (1970).
- ²⁴S. Friberg, C. K. Hong, and L. Mandel, *Phys. Rev. Lett.* **54**, 2011 (1985).
- ²⁵See for example B. E. Saleh, *Photoelectron Statistics* (Springer-Verlag, Berlin, 1978).
- ²⁶E. T. Whittaker and G. N. Watson, *A Course of Modern Analysis* (Cambridge University Press, London, 1973), pp. 134–139.